ELSEVIER

Contents lists available at ScienceDirect

# Journal of Power Sources

journal homepage: www.elsevier.com/locate/jpowsour



# Synthesis and electrochemical performance of cathode material Li<sub>1.2</sub>Co<sub>0.13</sub>Ni<sub>0.13</sub>Mn<sub>0.54</sub>O<sub>2</sub> from spent lithium-ion batteries



Li Li <sup>a</sup>, Xiaoxiao Zhang <sup>a</sup>, Renjie Chen <sup>a,\*</sup>, Taolin Zhao <sup>a</sup>, Jun Lu <sup>b</sup>, Feng Wu <sup>a</sup>, Khalil Amine <sup>b,1</sup>

<sup>a</sup> School of Chemical Engineering and the Environment, Beijing Institute of Technology, Beijing 100081, China

#### HIGHLIGHTS

- Re-synthesis of Li-rich cathode material Li<sub>1.2</sub>Co<sub>0.13</sub>Ni<sub>0.13</sub>Mn<sub>0.54</sub>O<sub>2</sub> from spent LIBs.
- Leaching solution from spent LIBs is successfully used as a source of Co and Li.
- $\bullet$  The re-synthesized material delivers a high initial discharge capacity of 258.8 mAh g<sup>-1</sup>.
- The high capacity retention of 87% can be obtained after 50 cycles.
- This technology can reduce the cost and realize cyclic utilization of spent LIBs.

#### ARTICLE INFO

# Article history: Received 20 July 2013 Received in revised form 28 September 2013 Accepted 21 October 2013 Available online 31 October 2013

Keywords: Spent lithium-ion battery Leaching solution Li-rich cathode material Oxalic acid co-precipitation

#### ABSTRACT

Li-rich layered oxide  $\text{Li}_{1.2}\text{Co}_{0.13}\text{Ni}_{0.13}\text{Mn}_{0.54}\text{O}_2$  has been successfully re-synthesized using the ascorbic acid leaching solution of spent lithium-ion batteries as the raw materials. A combination of oxalic acid coprecipitation, hydrothermal and calcination processes was applied to synthesize this material. For comparison, a fresh sample with the same composition has been also synthesized from the commercial raw materials using the same method. X-ray diffraction (XRD), scanning electron microscopy (SEM), X-ray photoelectron spectroscopy (XPS) and electrochemical measurements are carried out to characterize these samples. XRD results indicate that both samples have the layered  $\alpha$ -NaFeO<sub>2</sub> structures with a space group of R $\overline{3}$ m. No other crystalline phase was detected by XRD. The electrochemical results show that the re-synthesized and fresh-synthesized sample can deliver discharge capacities as high as 258.8 and 264.2 mAh g<sup>-1</sup> at the first cycle, respectively. After 50 cycles, discharge capacities of 225.1 and 228 mAh g<sup>-1</sup> can be obtained with capacity retention of 87.0 and 86.3%, respectively. This study suggests that the leaching solution from spent lithium ion batteries can be recycled to synthesize Li-rich cathode materials with good electrochemical performance.

Crown Copyright © 2013 Published by Elsevier B.V. All rights reserved.

#### 1. Introduction

Due to their favorable characteristics including high energy density, long cycle life and low self-discharge, lithium-ion batteries (LIBs) are widely used in portable electronic devices and electric automobiles [1,2]. The worldwide LIBs production had reached almost 4.6 billion in 2010 and is estimated to be 7.0 billion in 2015 [3,4]. Consequently, the end-of-life spent LIBs as well as waste battery materials generated during manufacturing process have increased tremendously, which is becoming an environmental

concern. Moreover, cobalt and lithium contained in the spent LIBs are important strategic metals which are extensively used in various fields [5]. The recycling of spent LIBs has, therefore, strong potential to provide environmental benefits in addition to conserving raw materials [6–8].

Layered LiCoO<sub>2</sub> is the most widely used cathode material in commercial LIBs, and the treatment and recycling of spent LIBs usually consist of two main steps: (1) acid leaching process to convert LiCoO<sub>2</sub> powder into solution; (2) using the leaching solution to produce new chemical products. In our previous work, we have developed an environmental friendly leaching process using organic acids to avoid secondary pollution with the similar efficiency as those using strong inorganic acids [9–11]. After leaching, the elements, mainly Co and Li, contained in the solution are usually recovered to new chemicals such as cobalt oxalate, lithium oxalate, cobalt hydroxide or cobalt oxide [5,12–14]. Other

<sup>&</sup>lt;sup>b</sup> Chemical Sciences and Engineering Division, Argonne National Laboratory, IL 60439, USA

<sup>\*</sup> Corresponding author. Tel.: +86 10 68912508.

E-mail addresses: chenrj@bit.edu.cn, chenrjbit@sina.com (R. Chen), amine@anl. gov (K. Amine).

<sup>&</sup>lt;sup>1</sup> Tel.: +1 630 2523838.

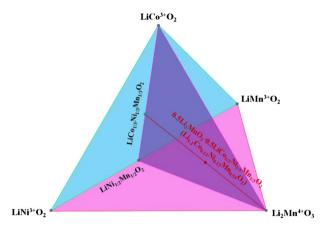


**Fig. 1.** Compositional phase diagram of the layered lithium transition metal oxide tetrahedron system: LiCoO<sub>2</sub>—LiNiO<sub>2</sub>—LiMnO<sub>2</sub>—Li<sub>2</sub>MnO<sub>3</sub>.

chemicals, for instance, microcrystalline lithium cobalt ferrite, nanocrystalline cobalt ferrite or  $\gamma$ -LiAlO<sub>2</sub>, can also be synthesized from the leaching solution [15–17]. Recovery of new active material LiCoO<sub>2</sub> or other electrode materials from the leaching solution are also under investigation, which is considered as a better way to achieve a sustainable LIB industry [18–21].

In order to replace the traditional LiCoO<sub>2</sub>, recent research effort of LIBs has been focused on the search of new cathode materials that have higher energy and power density, higher safety and lower cost. Li-rich manganese-based layered oxides, which are commonly described by the chemical formula of  $z\text{Li}_2\text{MnO}_3 \cdot (1-z)\text{LiMeO}_2$  (Me = Co, Ni, Mn, etc.) or reformulated as  $\text{Li}[\text{Li}_{x/3}\text{Me}_{1-x}\text{Mn}_{2x/3}](0 < x < 1)$ , have attracted significant attention because of their much higher capacity (>250 mAh g<sup>-1</sup>) with wider operating voltage windows (>3.5 V vs. Li/Li<sup>+</sup>) [22–26]. Among the various transition metal ratios, the composite  $\text{Li}_{1.2}\text{Co}_{0.13}\text{Ni}_{0.13}\text{Mn}_{0.54}\text{O}_2$ , with proportion of  $0.5\text{Li}_2\text{MnO}_3 \cdot 0.5\text{LiCo}_{1/3}\text{Ni}_{1/3}\text{Mn}_{1/3}\text{O}_2$  (labeled in Fig. 1) have been well studied by many researchers and proved to be an optimized composition with excellent electrochemical properties [26–30].

In this work, a combination of oxalic acid co-precipitation, hydrothermal and calcination processes was applied to re-

synthesize Li-rich manganese-based layered oxide  $\rm Li_{1.2}Co_{0.13}$ - $\rm Ni_{0.13}Mn_{0.54}O_2$  from the organic acid leaching solution of spent LIBs. For comparison, a fresh sample with the same composition has been also synthesized from the commercial raw materials using the same method. The structure, morphology, and electrochemical performances of both samples were investigated systematically.

#### 2. Experimental

# 2.1. Materials and reagents

The leaching solution was obtained from spent LIBs using ascorbic acid as leaching agent. The details of pretreatment and acid leaching process were described in our previous work [11]. All reagents used in this study were analytical grade, and all the solutions were prepared with distilled water.

## 2.2. Synthesis processes

 $Li_{1.2}Co_{0.13}Ni_{0.13}Mn_{0.54}O_2$  powder was re-synthesized through oxalic acid co-precipitation, hydrothermal and calcination processes, as illustrated in Fig. 2. Firstly, a desirable amount of leaching solution containing Co and Li was prepared after acid leaching process. Then, the stoichiometric amount of CH<sub>3</sub>COOLi·2H<sub>2</sub>O, Ni(CH<sub>3</sub>COO)<sub>2</sub>·4H<sub>2</sub>O and Mn(CH<sub>3</sub>COO)<sub>2</sub>·4H<sub>2</sub>O were dissolved in the leaching solution together, and the resulting solution is continuously stirred at room temperature for 0.5 h. Oxalic acid was added drop by drop into the mixed aqueous solution under stirring as a precipitating agent, which was then transferred into a sealed PTFE (Polytetrafluoroethylene) container followed by heating at 200 °C for 8 h. After the hydrothermal reaction, the mixture was stirred vigorously until dry at 80 °C. Finally, the dried powder was preheated in air at 450 °C for 5 h and then calcined in air at 900 °C for 12 h. The final product was obtained after uniform grinding. For comparison, the stoichiometric amounts of CH<sub>3</sub>COOLi·2H<sub>2</sub>O,  $Co(CH_3COO)_2 \cdot 4H_2O$ ,  $Ni(CH_3COO)_2 \cdot 4H_2O$  and  $Mn(CH_3COO)_2 \cdot 4H_2O$ were used as starting materials to synthesize Li<sub>1.2</sub>Co<sub>0.13</sub>-Ni<sub>0.13</sub>Mn<sub>0.54</sub>O<sub>2</sub> by the same method, and it was designated as freshsynthesized sample hereafter.

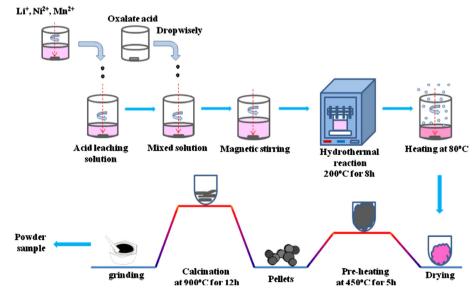


Fig. 2. Flow chart of Li<sub>1.2</sub>Co<sub>0.13</sub>Ni<sub>0.13</sub>Mn<sub>0.54</sub>O<sub>2</sub> re-synthesis process.

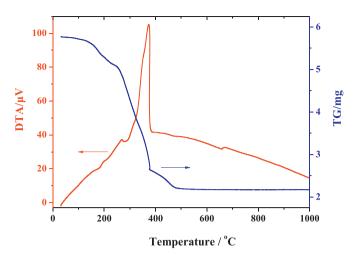


Fig. 3. TG/DTA curves of the re-synthesized  $Li_{1.2}Co_{0.13}Ni_{0.13}Mn_{0.54}O_2$  precursor.

#### 2.3. Material characterizations

The amount of Co and Li in the leaching solution was analyzed by AAS (Atomic Absorption Spectroscopy). Thermogravimetric and differential thermal (TG/DTA) analyzer was used to determine the appropriate calcination temperature for the precursor before calcination. The sample was heated from room temperature to  $1000\,^{\circ}\text{C}$  with a heating rate of  $10\,^{\circ}\text{C}$  min $^{-1}$  in air atmosphere.

The samples were characterized by X-ray diffraction (XRD, Rigaku Ultima IV-185) with a Cu- $K\alpha$  radiation source. Data were collected in the range of  $10-90^{\circ}$  at a scan rate of  $8^{\circ}$  min<sup>-1</sup>. The morphological and the elemental distribution of the samples were determined using FEI Quanata 200f scanning electron microscope (SEM) and Energy Dispersive X-ray (EDX) analysis. XPS measurement was conducted on a PHI QUANTERA-II SXM system (Japan/Uivac-PHI, INC), using a monochromatised Mg- $K\alpha$  radiation source.

Electrochemical performances of the samples were measured using galvanostatic cycling with two-electrode coin cells (type CR2025). The electrode was fabricated by coating the slurry of a mixture containing synthesized sample, acetylene black and polyvinylidene difluoride (PVDF) with a weight ratio of 8:1:1 onto circular aluminum current collector foils. Cells were assembled in an Argon-filled glove box, using the metallic lithium foil as counter electrode. The electrolyte was 1 M LiPF<sub>6</sub> dissolved in ethyl carbonate (EC) and dimethyl carbonate (DMC) (1:1 in volume) and the separator was Cellgard 2400 membrane. Charge and discharge experiments were performed on Land battery testers (Land CT2001A, Wuhan, China) with constant current condition between 2.0 and 4.8 V. The assembled cells were tested for 50 cycles at the current densities of 0.1 C (20 mA g<sup>-1</sup>) to analyze cycling performance. Various C rates (0.1, 0.2, 0.5, 1.0, and 2.0 C) were also tested to investigate the rate capability of the samples. Cycling at different temperatures (-20, 0, 30 and 60 °C) were tested to analyze the materials performance at high and low temperature. Cyclic voltammogram of the assembled cell was performed on the CHI electrochemical workstation (CHI660, Shanghai, China) at room

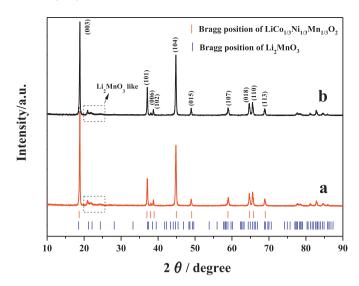


**Fig. 4.** XRD patterns of the synthesized samples: (a) the re-synthesized sample; (b) the fresh-synthesized sample.

temperature between 2 and 5 V at a sweep rate of 0.1 mV s<sup>-1</sup>. The potentials throughout the paper are in reference to Li/Li<sup>+</sup> couple.

#### 3. Results and discussion

# 3.1. TG/DTA analysis

TG/DTA scans of the precursor are shown in Fig. 3. Five distinct regions of weight loss were observed and the results are given in Table 1. A weight loss of 3.5 wt. % was detected from room temperature to 159 °C, resulting from the loss of absorbed water. The weight loss (8.6 wt. %) in the temperature range of 159 °C–247 °C was ascribed to the loss of the structural water in the sample. In the temperature region from 247 °C to 378 °C, there is a distinct weight loss of 41.96 wt. %, which corresponds to the decomposition of oxalates [5,31]. A weight loss of about 7.7% is observed in the range of 378 °C–480 °C due to the decomposition of acetates [32,33]. Finally, in the high temperature range from 480 °C to 1000 °C, a weight loss of 0.57 wt. % indicates the formation of Li<sub>1,2</sub>Co<sub>0.13</sub>-Ni<sub>0.13</sub>Mn<sub>0.54</sub>O<sub>2</sub> and the improvement of its crystallinity.

#### 3.2. XRD, SEM and EDX characterizations

The XRD patterns (Fig. 4) of the re-synthesized and fresh-synthesized  $\text{Li}_{1.2}\text{Co}_{0.13}\text{Ni}_{0.13}\text{Mn}_{0.54}\text{O}_2$  materials show that both samples have the layered structure without any impurity reflections. All the peaks can be indexed to a hexagonal  $\alpha$ -NaFeO<sub>2</sub> structure with a space group of  $R\overline{3}$ m, excluding the weak super-structure reflections around  $20-25^{\circ}$  that correspond to the ordering of Li and Mn in the transition metal layer of the layered lattice [27]. The weak superstructure reflections are characteristic of the integrated monoclinic Li<sub>2</sub>MnO<sub>3</sub>-like component (C/2m) [26].

SEM images of the re-synthesized and fresh-synthesized samples are shown in Fig. 5. No obvious differences between the two

**Table 1**TG data for the re-synthesized precursor.

	30−159 °C	159–247 °C	247–378 °C	378−480 °C	480-1000 °C
Weight loss wt%	3.5	8.6	41.96	7.7	0.57
Assignment	Loss of adsorbed water	Loss of structural water	Oxalates decomposition	Acetates decomposition	Li <sub>1.2</sub> Co <sub>0.13</sub> Ni <sub>0.13</sub> Mn <sub>0.54</sub> O <sub>2</sub> formation

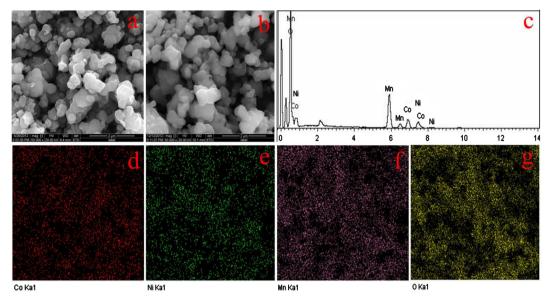


Fig. 5. SEM, EDX and elements distribution of the synthesized samples: (a) fresh-synthesized sample, (b) re-synthesized sample, (c) EDX, (d) Co distribution, (e) Ni distribution, (f) Mn distribution, (g) O distribution.

samples are observed from SEM observation. Both samples show smooth surface with well-distributed particles with the particle being smaller than 1  $\mu m.$  In addition, the composition, proportion and element distributions of the re-synthesized sample are investigated by EDX. The result shows that the re-synthesized sample consists of expected elements and the content of the different elements are well consistent with the stoichiometric ratio, as displayed in Table 2.

# 3.3. X-ray photoelectron spectra

The XPS spectra of the re-synthesized Li<sub>1.2</sub>Co<sub>0.13</sub>Ni<sub>0.13</sub>Mn<sub>0.54</sub>O<sub>2</sub> sample are shown in Fig. 6(a)—(d). As can be seen from Fig. 6(b), the Ni 2p spectrum exhibits four peaks. Two relatively intense signals at 855.6 and 873.3 eV are assigned to Ni 2p<sub>3/2</sub> and Ni 2p<sub>1/2</sub>. The Ni 2p<sub>3/2</sub> binding energy of 855.6 eV is in agreement with Ni<sup>2+</sup> in the literature [34]. The Co 2p spectrum is shown in Fig. 6(c). The binding energy for the Co 2p<sub>1/2</sub> and Co 2p<sub>3/2</sub> are at 795.1 and 780.4 eV, respectively, suggesting an oxidation state of Co<sup>3+</sup> [35]. Fig. 6(d) shows the Mn 2p spectra, and two major peaks with binding energies of 642 and 654 eV were observed, which are in good accordance with data for Mn<sup>4+</sup> [36].

# 3.4. Electrochemical performance

Fig. 7 shows the cycle properties and capacity retentions of the re-synthesized and fresh-synthesized Li<sub>1.2</sub>Co<sub>0.13</sub>Ni<sub>0.13</sub>Mn<sub>0.54</sub>O<sub>2</sub> samples between 2.0 and 4.8 V at 0.1 C. For the re-synthesized sample, a relatively fast capacity decay from 258.8 mAh g $^{-1}$  to 226.3 mAh g $^{-1}$  is observed in the initial 10 cycles. After that the discharge capacity maintains at 225.1 mAh g $^{-1}$  until the 50th cycle, showing a high capacity retention of 87% after 50 cycles. In comparison, the fresh-synthesized sample delivers discharge capacities of 264.2 mAh g $^{-1}$  at 1st cycle and 228 mAh g $^{-1}$  at 50th cycle with capacity retention of 86.3%. It can be seen that there is no visible difference between both samples in the capacity and cycle performances.

Charge/discharge profiles of 1st, 2nd, 5th, 10th, 20th and 50th cycle for the re-synthesized Li<sub>1.2</sub>Co<sub>0.13</sub>Ni<sub>0.13</sub>Mn<sub>0.54</sub>O<sub>2</sub> sample are shown in Fig. 8. The first charge curve shows two plateaus due to

the existence of two different lithium extraction processes [37]. The first plateau, which is positioned at  $\sim 4.0$  V, is associated to the delithiation of the  $LiMn_{1/3}Ni_{1/3}Co_{1/3}O_2$ -like region that corresponds to the oxidation of  $Ni^{2+} \rightarrow Ni^{4+}$  and  $Co^{3+} \rightarrow Co^{4+}$  [23]. The second plateau at ~4.5 V is widely accepted to originate from the simultaneous oxygen release with lithium deintercalation from the layered Li<sub>2</sub>MnO<sub>3</sub> lattice [37], which might be transformed to a MnO<sub>2</sub>-like phase. The capacity delivered during the first discharge resulted from the insertion of lithium in both the LiMn<sub>1/3</sub>Ni<sub>1/3</sub>Co<sub>1/</sub> <sub>3</sub>O<sub>2</sub>-like region and the MnO<sub>2</sub>-like region. The sample can achieve a charge capacity of 345.8 mAh g<sup>-1</sup> and a discharge capacity of 258.8 mAh g<sup>-1</sup> at the first cycle, implying the first Coulombic efficiency of 75%. After the first cycle, there is a remarkable change in the charge curve shapes of next cycles. The second plateau around 4.5 V disappears and Coulombic efficiency stabilizes at 99%.

In order to study the rate capability of the re-synthesized Li<sub>1.2</sub>Co<sub>0.13</sub>Ni<sub>0.13</sub>Mn<sub>0.54</sub>O<sub>2</sub> sample, the cells were discharged at various rates from 0.2 C to 5.0 C, respectively, and the results are shown in Fig. 9 and Table 3. As the applied current density increases, the discharge capacity of the sample decreases gradually due to the increasing polarization of the electrodes at higher current densities. The first discharge curves are presented in the internal of Fig. 9. The detailed data in Table 3 show that the initial discharge capacities of the re-synthesized sample can reach to 249 mAh g<sup>-1</sup> for 0.2 C, 237.8 mAh g<sup>-1</sup> for 0.5 C, 223.3 mAh g<sup>-1</sup> for 1 C, 218.1 mAh g<sup>-1</sup> for 2 C and 179.7 mAh g<sup>-1</sup> for 5 C. After 50 cycles, the discharge capacities at various rates drop to 193.9 mAh g<sup>-1</sup> for 0.2 C, 183.4 mAh g<sup>-1</sup> for 0.5 C, 168.2 mAh g<sup>-1</sup> for 1 C, 152.3 mAh g<sup>-1</sup> for 2 C and 126.2 mAh g<sup>-1</sup> for 5 C.

**Table 2**Molar ratio data of prepared Li[Li<sub>0.2</sub>Co<sub>0.13</sub>Ni<sub>0.13</sub>Mn<sub>0.54</sub>]O<sub>2</sub> measured by EDX.

Element	Molar ratio					
	Re-synthesized sample	Fresh-synthesized sample	Theoretical value (%)			
Co K	13.05	12.93	13			
Ni K	13.15	13.24	13			
Mn K	53.8	53.83	54			

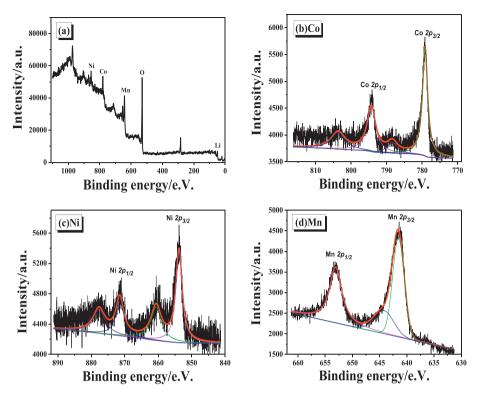


Fig. 6. X-ray photoelectron spectra of the re-synthesized sample: (a) Li-Co-Ni-Mn-O, (b) Co, (c) Ni, (d) Mn.

Another rate test was carried out to measure the rate capability of the re-synthesized and fresh-synthesized samples and the result is presented in Fig. 10. The average discharge capacities at 0.1 C, 0.2 C, 0.5 C, 1 C, 2 C of the re-synthesized sample are 256.6, 235.6, 206.4, 183.4 and 158.2 mAh g $^{-1}$ . About 87.7% (227 mAh g $^{-1}$ ) of the discharge capacity can be recovered once the rate is back to 0.1 C. Meanwhile, the fresh-synthesized sample shows the same trend as the re-synthesized sample, which delivers a little higher capacity at all rates.

In order to investigate the re-synthesized material performance at high and low temperature, the cells were discharged at -20 °C, 0 °C, 30 °C and 60 °C and the results are shown in Fig. 11 and Table 3. The discharge capacities are 139.1 mAh g<sup>-1</sup> at -20 °C, 210.5 mAh g<sup>-1</sup> at 0 °C, 260 mAh g<sup>-1</sup> at 30 °C and 271.3 mAh g<sup>-1</sup> at

3.5. Cyclic voltammogram Fig. 12 shows the CV curves of the re-synthesized sample at a slow sweep rate of 0.1 mV s $^{-1}$  in the voltage range of 2–5 V. There are two oxidation peaks at  $\sim$ 4.0 and  $\sim$ 4.6 V in the first charge

60 °C, respectively. It is clearly seen that the discharge capacity of

the sample increases with the increasing temperature. Meanwhile,

the discharge voltage presents gradually elevated trend with the

growth of temperature below 30 °C. However, there is a slightly

decrease of the discharge voltage from 30 °C to 60 °C, which maybe

due to the higher overpotential at high temperature.

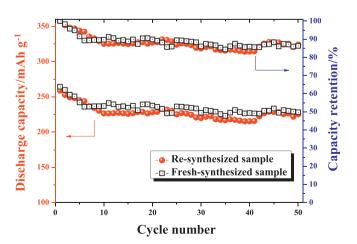


**Fig. 7.** Cycling performance and capacity retention comparison of the re-synthesized sample and fresh-synthesized sample at 0.1 C in the voltage range of 2–4.8 V.

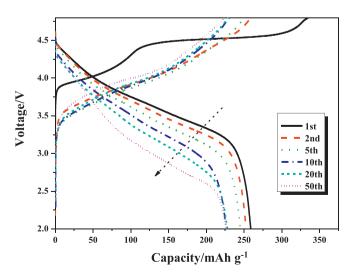


**Fig. 8.** Charge/discharge profiles of 1st, 2nd, 5th, 10th, 20th and 50th cycles of the resynthesized sample at 0.1 C in the voltage range of 2–4.8 V.

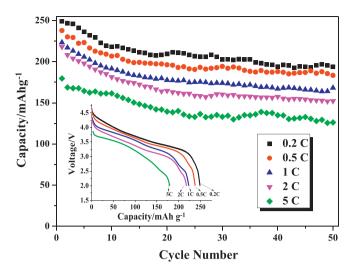


**Fig. 9.** Cycling performance of the re-synthesized sample  $\text{Li}/\text{Li}_{12}\text{Co}_{0.13}\text{Ni}_{0.13}\text{Mn}_{0.54}\text{O}_2$  cells charged at 0.1 C and discharged at different rates in the voltage range of 2–4.8 V.

**Table 3**Charge and discharge capacity, and capacity retention of the re-synthesized sample.

Temperature/°C	Discharge capacity/ mAh g <sup>-1</sup>	Rate	1st discharge capacity/ mAh g <sup>-1</sup>	50th discharge capacity/ mAh g <sup>-1</sup>	Capacity retention
-20 0 30 60	139.1 210.5 260 271.3	0.2 C 0.5 C 1.0 C 2.0 C	258.8 249 237.8 223.3 218.1 179.7	225.1 193.9 183.4 168.2 152.3 126.2	87.0% 77.9% 77.1% 75.3% 69.8% 70.2%

process, corresponding to the oxidation of the M components  $(M = Ni^{2+}, Co^{3+})$ , and the release of oxygen, respectively. In the first discharge process, there are three distinguishable reduction peaks at  $\sim$ 4.3,  $\sim$ 3.7 and  $\sim$ 3.3 V. The unconspicuous reduction peak at  $\sim$ 4.3 and the distinct reduction peak  $\sim$ 3.7 V are apparently attributed to the reduction of  $Ni^{4+}$  and  $Co^{4+}$ , while the peak at  $\sim$ 3.3 V can be associated to the reduction of  $Mn^{4+}$  triggered by the electrochemical activation of  $Li_2MnO_3$  in first charge process. From the second cycle, the CV features are significantly different

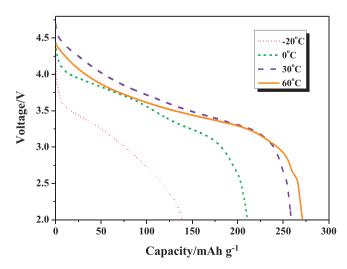


**Fig. 11.** First discharge profiles of the re-synthesized sample at -20, 0, 30 and 60 °C at 0.1 C in the voltage range of 2-4.8 V.

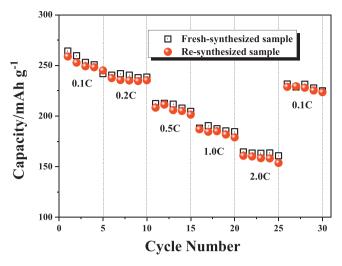


Fig. 10. Rate capability comparison of the re-synthesized sample and the fresh-synthesized sample in the voltage range of 2–4.8 V.

from those observed in the first cycle. The strongest oxidation peak at  $\sim$ 4.6 V disappears and a weak new peak emerges at  $\sim$ 4.5 V. The two oxidation peaks at  $\sim$ 3.9 V and  $\sim$ 4.5 V should be the oxidation of Ni<sup>2+</sup> and Co<sup>3+</sup>, respectively [38]. The reversible redox of Mn<sup>4+</sup>/Mn<sup>3+</sup> can still be observed below 3.5 V in the next scans. In addition, the oxidation peak of Mn<sup>3+</sup>/Mn<sup>4+</sup> appears and becomes stronger on cycling. Meanwhile, the position of the Mn<sup>4+</sup>/Mn<sup>3+</sup> peak in the discharge process shifts to the left gradually with cycles, which is associated with the structure transformation from layered to a layered-spinel intergrowth structure [39]. The high overlap extent of the cycle profiles demonstrates the good reversibility of the synthesized sample.

# 4. Conclusion

Li $_{1.2}$ Co $_{0.13}$ Ni $_{0.13}$ Mn $_{0.54}$ O $_2$  was successfully re-synthesized through oxalic acid co-precipitation, hydrothermal and calcination processes, using the acid leaching solution from spent lithiumion batteries. The re-synthesized sample showed the  $\alpha$ -NaFeO $_2$  structure with the R $\overline{3}$ m space group and the characteristic peaks of the Li $_2$ MnO $_3$  phase. The electrochemical results showed that the resynthesized sample achieved a charge capacity of 345.8 mAh g $^{-1}$ 

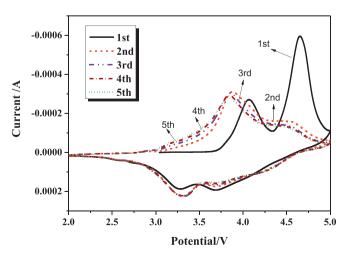


Fig. 12. Cyclic voltammogram of the re-synthesized sample.

and a discharge capacity of 258.8 mAh g<sup>-1</sup> at the first cycle at 0.1C, implying a Coulombic efficiency of 75%. It delivered a reversible discharge capacity as high as 225.1 mAh g<sup>-1</sup> and the capacity retention can be up to 87% after 50 cycles. The cycle performance and rate capability of the re-synthesized Li<sub>1.2</sub>Co<sub>0.13</sub>Ni<sub>0.13</sub>Mn<sub>0.54</sub>O<sub>2</sub> material was almost as good as that of fresh-synthesized material. The results showed that the leaching solution from spent LIBs can be used as a source of Co and Li elements to re-synthesize Li-rich cathode material. The technology developed in this study was environmentally friendly and could reduce the cost of cathode materials, realizing the cyclic utilization of spent LIBs finally.

#### Acknowledgments

The experimental work of this study was supported by the International S&T Cooperation Program of China (2010DFB63370), the Chinese National 973 Program (2009CB220106), Beijing Nova Program (Z121103002512029), Beijing Excellent Talents Plan Funding and the New Century Educational Talents Plan of the Chinese Education Ministry (NCET-12-0050). This work was also supported by the U.S. Department of Energy under Contract DE-AC0206CH11357 provided by the Vehicle Technologies Office, Department of Energy (DOE) Office of Energy Efficiency and Renewable Energy (EERE). This work especially thanks to US-China Electric Vehicle and Battery Technology between Argonne National Laboratory and Beijing Institute of Technology.

#### References

- [1] J. Nan, D. Han, X. Zuo, J. Power Sources 152 (2005) 278-284.
- [2] D.I. Ra, K.S. Han, J. Power Sources 163 (2006) 284–288.
- [3] B. Swain, J. Jeong, J.C. Lee, G.H. Lee, J.S. Sohn, J. Power Sources 167 (2007) 536—
- [4] UMICORE, Materials Technology Group, http://www.umicore.com (accessed 06.01.12).
- [5] L. Sun, K.O. Qiu, Waste Manag. 32 (2012) 1575-1582.
- [6] S. Catillo, F. Ansart, C. Laberty-Robert, J. Portal, J. Power Sources 112 (2002) 247-254.
- [7] J. Xu, H.R. Thomas, R.W. Francis, K.R. Lum, J. Wang, B. Liang, J. Power Sources 177 (2008) 512-527.
- [8] J.F. Paulino, N.G. Busnardo, J.C. Afonso, J. Hazard. Mater. 150 (2008) 843–849.
- [9] L. Li, J. Ge, F. Wu, R.J. Chen, S. Chen, B.R. Wu, J. Hazard. Mater. 176 (2010) 288-293

- [10] L. Li, J. Ge, R.J. Chen, F. Wu, S. Chen, X.X. Zhang, Waste Manag. 30 (2010) 2615-2621.
- [11] L. Li, J. Lu, Y. Ren, X.X. Zhang, R.J. Chen, F. Wu, K. Amine, J. Power Sources 218 (2012) 21-27.
- [12] L. Chen, X.C. Tang, Y. Zhang, L.X. Li, Z.W. Zeng, Y. Zhang, Hydrometallurgy 108 (2011) 80-86.
- [13] J. Kang, G. Senanayake, J. Sohn, S.M. Shin, Hydrometallurgy 100 (2010) 168-
- [14] I Kang I Sohn H Chang G Senanayake S M Shin Adv Powder Technol 21 (2010) 175–179.
- [15] L. Yang, O.H. Yan, G.X. Xi, I. Mater, Sci. 46 (2011) 6106–6110.
- [16] M. Bahgat, F.E. Farghaly, S.M. Abdel Basir, O.A. Fouad, J. Mater. Process. Technol. 183 (2007) 117-121.
- [17] O.A. Fouad, F.I. Farghaly, M. Bahgat, J. Anal. Appl. Pyrolysis 78 (2007) 65-69.
- [18] C.K. Lee, K.I. Rhee, J. Power Sources 109 (2002) 17–21.
- [19] L. Li, R.I. Chen, F. Sun, F. Wu, I.R. Liu, Hydrometallurgy 108 (2011) 220–225.
- [20] D.S. Kim, J.S. Sohn, C.K. Lee, J.H. Lee, K.S. Han, Y. Lee, J. Power Sources 132 (2004) 145-149.
- [21] D.W. Song, Y.N. Xu, C.H. An, Phys. Chem. Chem. Phys. 14 (2012) 71–75.
- [22] N. Yabuuchi, K. Yoshii, S.T. Myung, J. Am. Chem. Soc. 133 (2011) 4404—4419.
   [23] C.S. Johnson, J.S. Kim, C. Le fief, N. Li, J.T. Vaughey, M.M. Thackeray, Electrochem. Commun. 6 (2004) 1085-1091.
- [24] M.M. Thackeray, C.S. Johnson, J.T. Vaughey, N. Li, S.A. Hackney, J. Mater. Chem. 15 (2005) 2257-2267.
- [25] M.M. Thackeray, S.H. Kang, C.S. Johnson, J.T. Vaughey, S.A. Hackney, Electrochem. Commun. 8 (2006) 1531-1538.
- [26] C.S. Johnson, N.C. Li, C. Le fief, J.T. Vaughey, M.M. Thackeray, Chem. Mater. 20 (2008) 6095-6106.
- [27] J.H. Lim, H. Bang, K.S. Lee, K. Amine, Y.K. Sun, J. Power Sources 189 (2009) 571-575 [28] Q.Y. Wang, J. Liu, A.V. Murugan, A.J. Manthiram, J. Mater. Chem. 19 (2009)
- 4965-4972
- [29] Y. Wu, A.V. Murugan, A.J. Manthiram, Electrochem. Soc. 155 (2008) A635-A641
- [30] J.M. Zheng, Z.R. Zhang, X.B. Wu, Z.X. Dong, Z. Zhu, Y.J. Yang, Electrochem. Soc. 155 (2008) A775-A782.
- [31] D.P. Wang, I. Belharouak, G.W. Zhou, K. Amine, J. Electrochem. Soc. 160 (2013) A3108-A3112
- [32] I. Taniguchi, C.K. Lim, D. Song, M. Wakihara, Solid State Ionics 146 (2002) 239 - 247
- [33] J.C. De Jesus, I. Gonzalez, A. Quevedo, T. Puerta, J. Mol. Catal. A Chem. 228 (2005) 283-291.
- [34] A.N. Mansour, Surf. Sci. Spectra 3 (1994) 231-238.
- [35] K.M. Shaju, G.V.S. Rao, B.V.R. Chowdari, Electrochim. Acta 48 (2002) 145–151.
- [36] N. Treuil, C. Labrugere, M. Menetrier, J. Portier, G. Campet, A. Deshayes, J.C. Frison, S.J. Hwang, S.W. Song, J.H. Choy, J. Phys. Chem. B 103 (1999) 2100-2106.
- [37] J.S. Kim, C.S. Johnson, J.T. Vaughey, M.M. Thackeray, S.A. Hackney, Chem. Mater. 16 (2004) 1996-2006.
- [38] Z.H. Lu, J.R. Dahn, J. Electrochem. Soc. 149 (2002) A815-A822.
- A.R. Armstrong, M. Holzapfel, P. Novak, C.S. Johnson, S.H. Kang, M.M. Thackeray, P.G. Bruce, J. Am. Chem. Soc. 128 (2006) 8694-8698.